Acta Cryst. (1995). D51, 98–109

The Influence of Temperature on Lysozyme Crystals. Structure and Dynamics of Protein and Water

BY I. V. KURINOV* AND R. W. HARRISON

Department of Pharmacology, Bluemle Life Sciences Building, Thomas Jefferson University, 233 S. 10th Street, Philadelphia, PA 19107, USA

(*Received* 2 *July* 1993; *accepted* 8 *August* 1994)

Abstract

Lysozyme structures at six different temperatures in the range 95–295 K have been determined using X-ray crystallography at a resolution of 1.7 Å. The crystals at lower temperatures had a 7.4% decrease in the unit-cell volume. The volume change was discontinuous with the volume being near 238000 Å^3 from 295 to 250 K and about 220200 Å^3 below 180 K. The thermal expansion of the protein has been analyzed and shows anisotropy, which is correlated with local atomic packing and secondary-structure elements. The lysozyme structure at low temperature is nearly the same as that at high temperature, with only small relative translations and rotations of structure elements including a hinge-bending rearrangement of two domains. Because of a considerable increase of lattice disorder at low temperature dynamical analysis of internal motion is difficult. The analysis of structural and dynamical properties of well ordered protein-bound water has been carried out.

Introduction

Temperature is one of the major state variables of thermodynamics and is the easiest to change during a crystallographic experiment. To a large degree the structural, dynamical and functional properties of biopolymers are determined by temperature. Therefore, temperature dependences of structural and dynamical properties of proteins are studied by many physical methods. One of the more powerful physical methods of generating detailed structural information about proteins is X-ray crystallography. High-resolution X-ray crystallography provides a large amount of structural information that can be used to understand specific features of protein function and activity. The temperature dependence of the structure of lysozyme together with the analysis of the limited dynamical data is described in this paper. The temperature dependence of commonly used measures of protein structure such as radius of gyration and accessible surface area are also analyzed.

Detailed low-temperature X-ray diffraction studies of the structure and dynamics of myoglobin (Hartmann *et al.*, 1982; Frauenfelder *et al.*, 1987) and RNAase (Tilton, Dewan & Petsko, 1992) have been carried out. The studies of thermal-expansion processes were carried out, and structural differences as a result of temperatures changes were analyzed. One of the interesting features was a discontinuity in the change of the unit-cell parameters around 200 K. This change was associated with structural rearrangements in proteins. Anisotropic protein expansion accompanied by non-uniform increase of atomic mobility was found to be correlated with increasing temperature. However, specific features and quantitative results were different for the mainly α-helical myoglobin and the mainly β-sheet RNAase. Moreover, no conclusions were drawn about the temperature influence on protein-bound water, and RNAase low-temperature studies used protein crystals with cryoprotectors, whose influences on protein structure and packing are unknown.

In order to study protein-bound water and to see if the conclusions drawn from the studies on RNAase and myoglobin were transferable to proteins in general, another protein was chosen. Lysozyme was chosen partially because high-quality large crystals of lysozyme may be grown easily and the crystals diffract to high resolution. It was already known (Young, Dewan, Thomson & Nave, 1990) that lysozyme crystals are suitable candidates for low-temperature studies using the shock-freezing technique. Lysozyme is well characterized both by X-ray crystallography (Blake *et al.*, 1965; Artymiuk *et al.*, 1979; Blake, Pulford & Artymiuk, 1983; Kundrot & Richards, 1987; Clarage, Clarage, Phillips, Sweet & Caspar, 1992) and by many other methods (for review see, McKenzie & White, 1991; Rupley & Careri, 1991). In particular, lysozyme has been a major model system for studying protein hydration (Rupley, Gratton & Careri, 1983; Teeter, 1991).

The X-ray analysis of structural and dynamical properties of lysozyme in the range 95–295 K is

* On leave from Institute of Chemical Physics, Moscow, Russia.

ISSN 0907-4449

described here. The overall influence of the temperature both on the protein and strongly bound ordered water is explored and discussed.

Experimental

Crystal preparation and data collection

Hen egg-white lysozyme (Sigma, Lot No. 89F8276) was used without further purification. Tetragonal crystals were obtained, as reported previously (Steinrauf, 1959), using hanging-drop experiments with 0.1 *M* sodium acetate and 5% NaCl stock solution (pH = 4.7) at room temperature. Lysozyme crystals about 0.8 mm in their largest dimension were used. For temperatures above 250 K the crystals were mounted in a thin glass capillary, with excess mother liquid removed.

Low-temperature studies were planned using both cryosolvent and shock freezing, in order to study the effects of altered solvents as well as the temperature. The preparation of lysozyme crystals with the cryoprotector, 2-methyl-2,4-pentanediol (MPD), as recommended by Petsko (Petsko, 1975) was tried. Two different possibilities were explored, growing the protein crystals from a stock solution containing small amounts of MPD and a stepped transfer of crystals from initial mother liquid to a final solution with 70% MPD. It is possible to grow lysozyme crystals with MPD concentrations up to 15% at room temperature and up to 20% at 278 K. Unfortunately, these crystals were not good enough for high-resolution crystallography even at room temperature. Slow transfers of crystals to MPD-containing solutions both at 278 K and room temperature failed. The crystals usually disintegrated.

Therefore, the method of shock-freezing (Dewan & Tilton, 1987; Hope, 1988, 1990) was used. For all low-temperature data sets, crystals were fixed on the tip of a thin glass fiber by a ball of epoxy cement. The crystal surface was carefully dried with filter paper, and the mounted crystal was quickly immersed in liquid nitrogen and, some minutes later, very quickly mounted on the diffractometer goniometric head under a cold nitrogen stream (T = 90 K). The temperature of the gas stream was slowly increased to the required value. The temperature of the gas stream near the crystal was checked with independent thermocouple prior to data collection to ensure that the crystal temperature was correctly recorded. Crystals mounted in this manner did not develop a coating of frost and diffracted to 1.7 Å resolution, but they showed an increase in mosaic spread. The total contribution of geometrical collimation, divergence of X-ray beam and real mosaic spread of the crystal could reach 1°. The protein crystals were stable and did not show radiation decay at low temperatures. The difference in integrated reflection intensities before and after measurement of full oscillation data sets (nearly one day of radiation exposure) did not exceed 5% for both low- or high-resolution regions and was probably due to systematic errors. When shock-frozen crystals were warmed above 200 K, the crystals became opaque, diffracted only to 3.5 Å resolution and diffraction disappeared rapidly. This feature deserves separate discussion in connection with possible roles of melting of protein-bound water and the emergence of fast relaxation processes in hydrated proteins (Doster, Cusack & Petry, 1989; Frauenfelder, Parak & Young, 1988).

Table 1. *Details of data collection*

Temperature (K)		95	120	180	250	280	295
Total No. of measured reflections		34658	25732	26287	34846	22932	29350
Completeness of data ($\sigma > 1$)	2.0 Å	87.2	88.5	85.9	91.8	80.6	94.3
	1.7 Å	75.6	75.3	77.5	83.1	79.8	77.7
No. of independent reflections ($\sigma > 2$)		9785	9792	10032	12186	10414	10142
R_{merge} (%)		7.64	7.88	5.45	9.31	5.08	4.58
a (Å)		76.996	77.008	77.020	79.069	79.244	79.245
c (Å)		37.132	37.237	37.034	37.826	37.935	37.858

Data were collected on an Rigaku R-AXIS 2 diffractometer with an image-plate detector. The imaging plate was placed at a distance of 100 mm from the lysozyme crystal with a detector angle of 10°. An X-ray data set was collected from a single crystal upon rotation of 60–80° (30–40 oscillation frames). The range was chosen with an oscillation simulation program to ensure maximal coverage of reciprocal space. Graphite-monochromatized Cu $K\alpha$ radiation was produced using a fine-focus Rotaflex RU-200BH rotating-anode X-ray generator operated at 50 kV and 100 mA. The diffractometer was equipped with a liquid-nitrogen refrigeration fixed-tube low-temperature system, which had been mounted in a fixed position on the diffractometer above the sample and produced a stream of cold nitrogen of controlled temperature, surrounded by a warm flow to prevent frosting around the sample and the goniometer head. A high-speed two-dimensional scan system was employed for image-plate reading. The read data were rapidly transferred to a VAXstation 3100, which performed the data processing. The data-processing software determines crystal orientation, integrated intensities, scaling and merging. A summary of data collection and processing for all samples studied is given in Table 1. To make accurate and comparable unit-cell measurements the data were first collected at room temperature and then the detector was not moved. This gave us an accurate film-to-crystal distance which was used in the temperature-shift experiments.

Table 2. *Summary of refinement details*

Temperature (K)	95	120	180	250	280	295
Final R factor	0.213	0.209	1.99	0.195	0.199	0.191
R.m.s.d. bonds (Å)	0.016	0.016	0.015	0.014	0.015	0.015
R.m.s.d. angles (°)	3.08	3.24	2.95	2.85	2.77	3.01
R.m.s.d. dihedrals (°)	22.8	22.8	22.9	23.7	22.7	23.6
R.m.s.d. impropers (°)	1.61	1.74	1.51	1.64	1.56	1.62
Total No. of waters in calculation	119	127	122	105	96	99
No. of waters						
with $B > 50$	8	22	10	19	17	20
with $B > 60$	2	4	1	11	3	2
No. of protein atoms with $B > 50$	5	—	1	—	—	—

Refinement of protein structure

The starting model was the lysozyme structure refined by Kundrot & Richards (1987) from the Protein Data Bank (Bernstein *et al.*, 1977), reference number 2LYM. All water molecules were removed from the initial model. A rigid-body R-factor minimization of this model was performed using the crystallographic refinement program *X-PLOR* (Brünger, 1992*a*). In addition to fitting the crystallographic data, intermolecular interactions between symmetry-related molecules were taken into account. The resulting structure was further refined using slow-cooling annealing with the *X-PLOR* package (Brünger, Krukovskii & Erickson, 1990; Brünger, 1992*a*). Initially an overall group temperature factor was used. Later in the refinement individual temperature factors were used. After the first cycle of simulated annealing, difference electron-density maps with coefficients $2|F_o| - |F_c|$ and $|F_o| - |F_c|$ were used as guides for manual changes in the model and the inclusion of solvent molecules using the program *FRODO* (Jones, 1985) on an Evans & Sutherland ESV10 computer graphics workstation. Special attention was paid to amino acids with long side chains. Sometimes they protruded into the solvent and occupied electron density from solvent molecules, rather than their own.

A modified annealing protocol was found to be most reliable. After the second cycle of electron-density inspection and addition of water molecules to the crystal structure, the final slow-cooling algorithm was run. Water molecules were weakly fixed to their position with harmonic restraints to prevent long-range diffusion at high temperature, and the relative weight of the X-ray term was increased by 60–80% from the ideal one, based on the equal gradient in order to ensure better convergence to electron-density peaks. After slow-cooling annealing, 3–4 energy-minimization steps with refinement of individual temperature factors were run with a steeply decreasing relative weight of the X-ray term in order to reach good stereochemistry. At the end of this protocol no manual intervention was necessary and the electron-density map had no uninterpretable features. The 'free-R test' (Brünger, 1992*b*) was performed for two structures at 95 and 295 K. In both cases the free R factor was no more than 9% higher than the resulting R factor. Results of the refinements are presented in Table 2. All structure-refinement calculations and model analysis were performed on a CONVEX C240 supercomputer.*

Results and discussion

Analysis and discussion of low-temperature data is divided into three parts. Part I deals with the influence of temperature on the protein structure, average structural properties and changes in protein packing. Part II explores some problems of protein dynamics and crystal disorder. Part III presents some preliminary results on water structure and behavior.

I. *Structural properties*

Lysozyme crystals used in low-temperature studies belong to the tetragonal space group $P4_32_12$ with a single molecule in the asymmetric unit. Unit-cell parameters determined for six different temperatures are shown in Fig. 1. These show a dramatic influence of temperature on the protein crystal. Note the difference in scales for the a and c axis changes with temperature. The total volume decrease going from high to low temperature is about 7.4%, and the corresponding volume change is 17600 Å^3 per unit cell. Despite the sparse sampling of data, it is clear that the temperature dependence of unit-cell parameters is non-linear and some transition occurs both in a and c dimensions of the unit cell in the region 200–230 K. This change is a direct consequence of the phase transition in protein–water systems that has been observed in this temperature range and connected with changes in structural and dynamical properties. The evidence of such a phase transition has been provided by many other physical methods (Rupley *et al.*, 1983; Frauenfelder *et al.*, 1988; Doster *et al.*, 1989; Krupyanskii, Goldanskii, Kurinov & Suzdalev, 1990).

The observed unit-cell volume change is larger than the one found for RNAase (4.7%) (Tilton *et al.*, 1992) and myoglobin (5.2%) (Frauenfelder *et al.*, 1987). This larger change could be due to a looser molecular packing in the unit cell, possibly with a smaller number of intermolecular interactions. The packing and space group are different than those of

* Atomic coordinates and structure factors have been deposited with the Protein Data Bank, Brookhaven National Laboratory (Reference: 1LSA, 1LSB, 1LSC, 1LSD, 1LSE, 1LSF, R1LSASF, R1LSBSF, R1LSCSF, R1LSDSF, R1LSESF, R1LSFSF). Free copies may be obtained through The Managing Editor, International Union of Crystallography, 5 Abbey Square, Chester CH1 2HU, England (Reference: GR0268).

RNAase and myoglobin, so that it is dangerous to assign a specific cause to this difference in volume change.

The volume change of the unit cell could be caused by the following factors: (1) as a result of usual thermal expansion of a substance (protein and water); (2) as a result of changes in intramolecular packing and orientation of protein molecules and (3) as a result of a structural transitions inside the protein molecule and of water rearrangement around protein. It will be shown that all the above factors are responsible for the observed unit-cell contraction.

Structure differences. A direct comparison of low- and high-temperature structures shows that the overall structure of lysozyme remains unchanged with freezing – Fig. 2 illustrates relative orientation of protein molecule in unit cell at LT and HT.* After rigid-body rotation and translation both backbones are nearly identical. However, there are structural differences even between structures which are close in temperature. These differences are largest in the regions that do not form regular elements of defined secondary structure. Fig. 3 shows a representative dependence of root-mean-square deviations in atomic coordinates for the lysozyme structures refined at 95 and 295 K. All other dependences are quite similar to this. Fig. 4 illustrates a clear example of conformational reorientation of a large amino acid. Trp62 has the same distribution of conformations at all temperatures above 250 K, with the electron density of Cz and Cε atoms poorly defined. In the LT structures this tryptophan was found to be more ordered in a different conformation.

Table 3 presents overall root-mean-square deviations (r.m.s.d.) for side-chain and main-chain atoms after best fitting (translational and rotation of the whole molecules) based on the superpostion of main-chain atoms. The low-temperature structures differ insignificantly with r.m.s.d for the main chain near 0.25 Å, whereas the LT and the HT structures differ by about 0.45 Å and the r.m.s.d. increase as the temperature difference increases. The largest

* LT - the average was performed on two structures at 95 and 120 K; HT - the average of 280 and 295 K structures. Difference between LT and HT structures are significantly larger than between two LT or two HT structures.

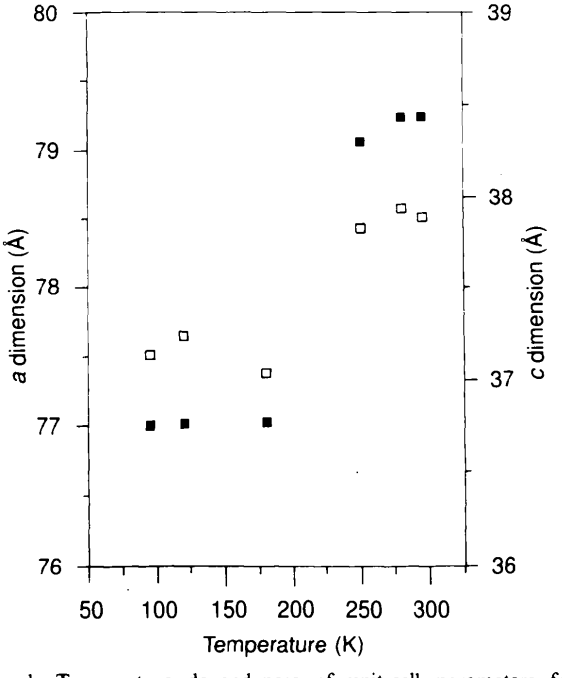

Fig. 1. Temperature dependences of unit-cell parameters for lysozyme crystals: ■, *a* dimension and □, *c* dimension (Å).

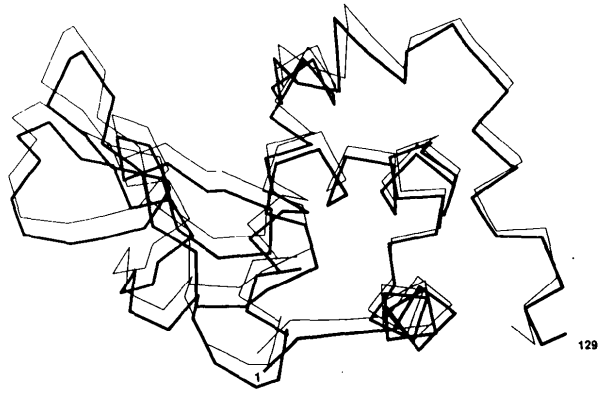

Fig. 2. Backbone Cα drawing of lysozyme structure at 95 K (thick line) and at 295 K (thin line). The magnitude of the rigid-body displacement is clearly illustrated.

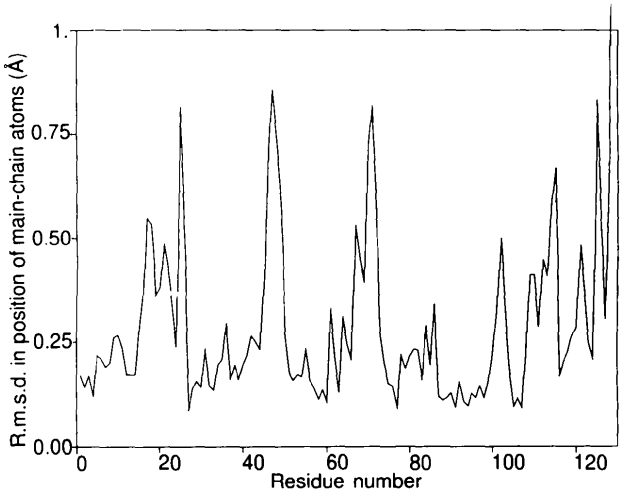

Fig. 3. A representative root-mean-square deviations between two lysozyme structure at 95 and 295 K averaged for main-chain atoms, after a best fit (including a translation and a rotation of whole structure) was performed. All other dependences look similar.

differences were observed for side chains, and they are nearly independent of the temperature, with the exception of 280 and 295 K. It is obviously necessary to consider the significance of these results. The maximum value of errors in the positions of heavy atoms was estimated from Luzzati plots (Luzzati, 1959) to be in the range of 0.2–0.25 Å coordinate error for all structures. The difference between structures obtained with slightly different refinement protocols (different weight of X-ray term, unit-cell parameters, *etc.)* was always less than 0.15 Å for main-chain atoms and about 0.4 Å for side-chain atoms in accordance with Kuriyan *et al.* (Kuriyan, Karplus & Petso, 1987).

During the structure comparison, it was very hard to find any systematic dependence of side-chain behavior connected with the temperature changes. Probably such larger r.m.s.d. for side chains were caused by adaptation to the new unit cell and by the freezing of differing conformations of long side chains. Therefore, most attention was paid to the behavior of the secondary-structure elements. In the protein molecule, seven well defined elements were considered: α-helices (residues 4–16, 24–36, 88–101, 119–124), β-strands (residues 42–46, 50–54, 57–60), the region of 61–87 and the C-terminal region 124–129. The full difference table is very cumbersome and is not visually informative. The main conclusions that were drawn concern anisotropic changes in the position of elements of secondary structures with temperature, and that those regions in which there are large random deviations between structures form loops, turns or termini. Direct comparison of the elements mentioned above is more illustrative when, to further reduce errors, the averaging of low- (95 and 120 K) and high-temperature (280 and 295 K) data was carried out (Table 4). All secondary elements, with the exception of the 24–36 helix, are conserved with an r.m.s.d. of less than 0.2 Å for main-chain atoms. However, the angle of rotation of each element needed to obtain the best superposition after their centres of mass were adjusted varies. From Table 4, it is clear that the β-sheet conserves its relative position in the unit cell as the temperature changes, while other elements need to be rotated by 2.6–3.5°. These changes strongly support the idea of anisotropic thermal expansion of the protein molecule.

Table 3. *Root-mean-square deviations* (Å) *between lysozyme structures at different temperatures*

Upper values correspond to main-chain atoms, lower to side-chain atoms excluding δ- and ε-atoms.

Temperature (K)	295	280	250	180	120	95
295		0.171	0.292	0.404	0.445	0.445
		0.684	0.884	1.019	1.040	1.051
280			0.296	0.432	0.455	0.473
			0.555	0.691	0.740	0.734
250				0.374	0.303	0.365
				0.562	0.477	0.566
180					0.308	0.247
					0.451	0.268
120						0.235
						0.409

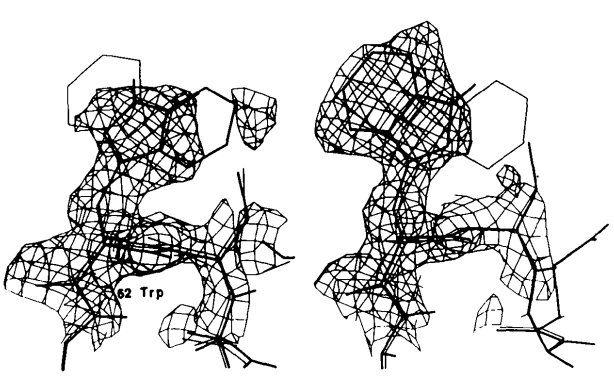

(*a*) (*b*)

Fig. 4. An increase in the ordering of the protein is seen when the temperature is lowered, even though the effective thermal factor remains unchanged. The most dramatic example of this is Trp62, which is disordered at room temperature and ordered at low temperatures. (*a*) Electron-density map of lysozyme structure at 295 K. Atomic models of lysozyme are superimposed as a thick line (295 K structure) and thin line (95 K structure). (*b*) Electron-density map of lysozyme structure at 95 K. Atomic models of lysozyme are superimposed as a thick line (95 K structure) and thin line (295 K structure). The maps were calculated with coefficients $2|F_o| - |F_c|$ and phases from the calculated structure factors of the corresponding atomic models. Residue Trp62 has been omitted for the calculation of $|F_c|$. Maps were contoured at 1σ.

Hinge-bending motion. It is well known that lysozyme is a two-domain protein. The cleft, containing the active center, lies between two lobes. A proposed hinge-bending motion which would be related to enzyme function (Janin & Wodak, 1983) has been analyzed by theoretical and experimental studies. Therefore, an attempt was undertaken to find the relative domain movement as a result of temperature changes. Two values were estimated: the relative distance between the centres of mass of the two domains and the difference in the rotation angle need to obtain the best superposition of each separate domain to its position in the LT structure. It was found that the relative domain separation decreased by 0.32 Å as the temperature decreased, which is nearly the same as the average found for other secondary elements. The angles of rotation for best-fitting independent domains differ by 1.75°. This result clearly indicates that the temperature change leads to closer proximity of the domains.

Intermolecular contacts. In addition to the structural changes inside the protein, the intermolecular crystal contacts were changed. Here a contact is

Table 4. *Parameters specifying difference in orientation between elements of secondary structure averaged for low- and high-temperature structures*

	Elements of secondary structure				
Residues	4–16	24–36	88–101	119–124	β-sheet
Rotation	2.6	3.2	3.5	2.9	1.2
Translation (Å)	2.01	2.01	1.81	1.73	2.02
R.m.s.d. (Å)	0.14	0.30	0.18	0.15	0.19

Table 5. *Number of intermolecular contacts (distance between symmetry-related molecules) in different shells as a function of temperature*

	Temperature (K)							
Distance (Å)	95	95*	95†	120	180	250	280	295
< 3.0	11	30	70	13	12	11	9	9
3 3.5	34	52	74	44	31	27	25	28
3.5 3.75	48	65	59	57	54	41	34	29
3.75–4.0	73	56	69	67	64	43	42	48
4.0–4.25	76	73	89	69	71	49	62	67
4.25 4.5	92	93	114	91	97	71	73	66

* The structure for 295 K was inserted in the 95 K unit cell after rotation and translation.

† As at 95 K but with the initial orientation.

defined as a close distance between nearest non-H atoms that belong to different protein molecules. To analyze the influence of temperature on protein packing, the numbers of all possible intermolecular contacts in different shells of contact distances were calculated for eight symmetry-related molecules (Table 5). The number of contacts less than 3 Å is nearly independent of the temperature and most remain unchanged with temperature. These contacts are probably responsible for the maintenance of the crystal lattice. All other contacts with distances of up to 4.5 Å become slightly more numerous at low temperatures. Additional stability of a low-temperature structure could come from more ordered water molecules, which creates additional strong water–protein contacts.

To determine whether the changes in the unit-cell dimensions influence protein structure we put the HT structure into the LT unit cell. Many energertically unfavorable contacts appear with distances less than 2 Å and the number of other contacts increased by a factor of two (see Table 5). It was found that the majority of these unfavorable contacts came from water molecules, so a rearrangement of the water structure is required. The protein molecules are translated by 1.9 Å and rotated by 2.4° from the room-temperature structure when the low-temperature structure is formed. The relative sliding and pivoting of the monomers occurs to form a more dense packing at low temperature. However some unfavorable contacts remain after rigid-body adjustment. Finer adjustments of surface side chains are needed to fit the low-temperature data. Thus, the temperature changes in protein structure appear correlated with the unit-cell modifications, since the unit-cell contraction does not lead to considerable increases in the number of intermolecular contacts in the refined structure.

Thermal expansion. The thermal contraction of the unit cell because of a simple linear thermal expansion can be easily estimated. It would lead to nearly linear temperature dependence of volume, unlike the experimental observations (Fig. 1). The linear thermal expansion coefficient for lysozyme measured in the range 298–323 K lies in the region of 1.35×10^{-4} K^{-1} (Bull & Breese, 1973). A 200 K temperature difference will result in protein volume changes of 8% with this coefficient. The volume of the unit cell is 237 930 Å^3 at 295 K, 236 485 Å^3 at 250 K and 220 130 Å^3 at 95 K. The corresponding observed thermal expansion coefficients are $\simeq 0.45 \times 10^{-4}$ K^{-1} for 295 to 250 K and $\simeq 1.2 \times 10^{-4}$ K^{-1} for 295 to 95 K. It must be noted that the thermal expansion is not uniform and, therefore, these coefficients are qualitative at best.

The thermal expansion of the protein can be parameterized in terms of the radius of gyration, $R_g = [\langle (r_i - \langle r_i \rangle)^2 \rangle]^{1/2}$. Since the radius of gyration is proportional to moment of inertia it gives a rough estimation of protein volume. Its values, calculated for both main-chain atoms and for all atoms are presented in Fig. 5. The radius of gyration decreases

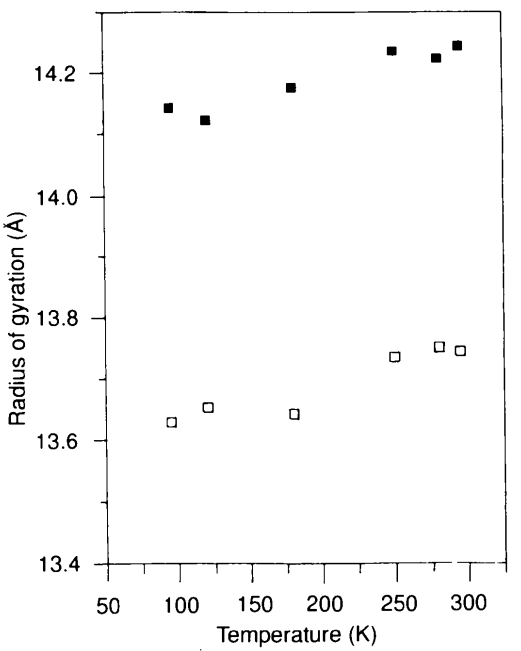

Fig. 5. Temperature dependence of radius of gyration, R_g (Å) for lysozyme: in calculations all atoms were used ■, or only main-chain atoms □.

by about 0.8% on going from 295 to 95 K (this corresponds to a 2.5% decrease of the volume of appropriate ellipsoid). Unlike the unit-cell dimension the radius of gyration shows a nearly linear contraction. The corresponding thermal expansion coefficient is $\simeq 0.4 \times 10^{-4}\,K^{-1}$ which is considerably smaller than the solution value. This is not completely surprising as the solution value will reflect the solvent–lysozyme interactions which are not present in the crystal.

Thermal expansion of lysozyme in the low-temperature region and in the crystal environment is less than in the solution and is only responsible for a small (around 2%) volume decrease with temperature on going from 295 to 95 K. In Fig. 1 the slope of the dependence of the cell volume on temperature is about 2% on either side of the phase transition suggesting that in the absence of a phase transition thermal expansion accounts reasonably well for the change in volume.

From the positions of non-H atoms it is possible to obtain a more detailed estimation of protein expansion based on the analysis of interatomic distances in the protein. It has been found (Frauenfelder *et al.*, 1987) that the fractional changes in distance between two atoms at different temperatures $\alpha(T_1,T_2)$ can be defined by,

$$\alpha(T_1, T_2) = \frac{[\langle r_{ij}(T_2) - r_{ij}(T_1)\rangle]}{(T_2 - T_1)\langle r_{ij}\rangle},$$

where r_{ij} is the distance between i and j atoms. Since the position of the main-chain atoms in a protein structure are usually the best determined, only the relative distances between $C\alpha$ and all atoms will be used. The results of these calculations are presented in Fig. 6. There are clearly local changes in protein structure as a result of the temperature increase. The largest expansions are located in the disordered region of protein, although some atoms inside α-helices also show a high value of $\alpha(T_1,T_2)$. There are some negative values of $\alpha(T_1,T_2)$, which correspond to thermal contraction between atoms as the temperature increases. No correlation of $\alpha(T_1,T_2)$ with the behaviour of the temperature factor or the accessible surface area for each residue was found. Thus, the non-uniform distribution of $\alpha(T_1,T_2)$ in Fig. 6 is a direct illustration of the anisotropic nature of thermal protein expansion both in the protein core and at the protein surface. Calculating the linear expansion coefficient for all atoms and averaging yields $4 \times 10^{-5}\,K^{-1}$. This value only a little lower than that for myoglobin $5 \times 10^{-5}\,K^{-1}$ (Frauenfelder *et al.*, 1987). So, the overall thermal expansion of lysozyme does not differ considerably to that of α-helical myoglobin.

Thermal protein expansion is also reflected in the changes in numbers of interatomic distances between different atom pairs. At low temperature protein atoms have more interatomic distances with values less than 21 Å and the thermal expansion of lysozyme is determined by decreasing the number of interatomic distances less than 21 Å, and by increasing the long-range (greater than 22 Å) distances at high temperature. It is evident that atoms separated by more than 21 Å are situated, mainly, near the protein surface and their relative motions are responsible in part for protein thermal expansion. The decrease in the number of short-range distances simply signifies the increase of interatomic volume at subatomic level, since no large internal cavities in protein at high temperature were found.

Surface area. Fig. 7 shows the accessible surface area, determined using a probe sphere of 1.6 Å radius. The behavior of the surface area is surprising because of its near independence of temperature. This is quite different from the data reported for RNAase and myoglobin (Tilton *et al.*, 1992; Frauenfelder *et al.*, 1987). The accessible surface area reflects the internal protein volume as long as the overall protein structure does not differ. However, if only a few long amino-acid side chains from the surface change conformation and produce into the solvent then the accessible surface will increase considerably, but the radius of gyration will show little change. For example, the accessible surface area for residues in the range 124–129 decreased by 17%, as the temperature increased from LT to HT averaged structures. So, the temperature dependence of surface area suggests two coexistent processes occurring as the temperature decreases: the overall anisotropic shrinking of the molecule and the increase of surface roughness. Some of the differences between these results and RNAase and myoglobin may also be due

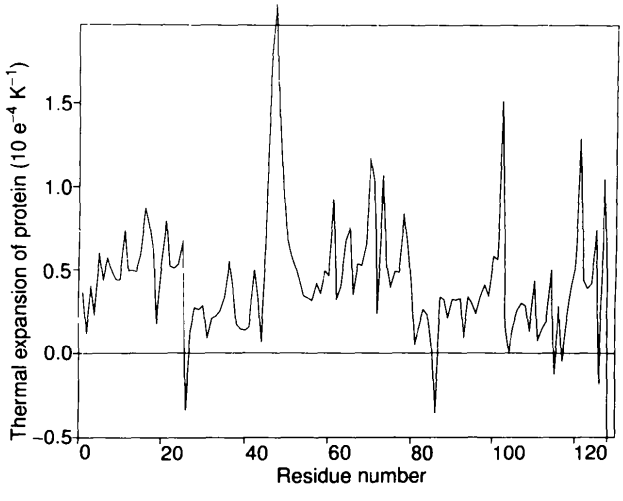

Fig. 6. Average thermal expansion coefficient of protein, $\alpha(T_1, T_2)$ $\times 10^{-4}\,K^{-1}$, as a function of residue number.

to ill defined aspects of calculating accessible surface area. For example, changing the probe radius can change the results in a non-uniform manner.

Strain analysis. All the considerations above are usual for structure comparison, but they ignore possible local deformations. Recently, a general method of using elastic deformations to describe structural changes was proposed (Andrews & Harrison, 1991). By analyzing the deformation of small portions of main chain (up to ten residues) it is possible to find regions where some distortion from rigid-body fitting of two structures occurs. The application of this method is illustrated in Fig. 8, where three eignenvalues of the strain tensor are plotted for comparison of the high- and low-temperature structures. The places where eigenvalues differ from unity indicate large deformations in the local structure. However, even though these values did not exceed 0.05 (for comparison: deoxy- and carbonmonoxyhemoglobin had shown values up to 0.2), they clearly show the regions of moderate local deformation in the lysozyme structure which are due to the temperature change.

Thus, the overall effect of the temperature on protein structure is the alteration of the packing of protein molecules inside the unit cell, accompanied by the translation and rotation of the protein as a whole, an anisotropic relative movement of secondary-structure elements, and a fine adaptation of disordered regions and of individual residues to the unit-cell changes.

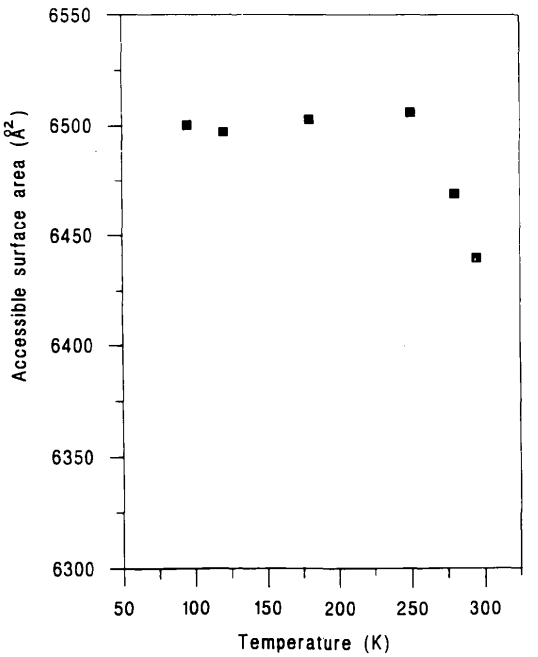

Fig. 7. Temperature dependence of calculated accessible surface area (Å²) of lysozyme, using a 1.6 Å radius probe.

II. *Dynamics*

Methods of X-ray crystallography are not suitable for quantitative studies of protein dynamics due both to the incompleteness and relative low resolution of experimental data (only isotropic temperature factor can be determined) and to the averaging of experimental results over long measurement time. The former reason leads to the neglect of the anharmonic and anisotropic nature of internal motions (Kuriyan, Petsko, Levy & Karplus, 1986), and the latter causes an inability to discriminate between real motions and static disorder (Petsko & Ringe, 1984; Kuriyan & Weis, 1991; Clarage *et al.*, 1992).

The main manifestation of protein dynamics is the smoothness and disappearance of observed electron density. This disappearance can be because of the presence of alternative conformations, local atomic disorder, differences in protein packing in the unit cell and imperfectness of the whole protein crystal. Usually, the diffuseness of electron density has been described qualitatively by the isotropic Debye–Waller factor: $B = 8\pi^2\langle x^2\rangle = 8\pi^2(\langle x^2\rangle_{ld} + \langle x^2\rangle_d)$, where $\langle x^2\rangle_d$ is the dynamical term determined by real motions and $\langle x^2\rangle_{ld}$ is the contribution of lattice and static disorder. In principle, from the temperature dependence of Debye–Waller factors, one can estimate the relative contribution of $\langle x^2\rangle_{ld}$ and $\langle x^2\rangle_d$, and Petsko & Ringe (1984) and Frauenfelder *et al.* (1987) concluded that internal motions have a dominant contribution in the temperature factor.

The overall temperature-factor values for side-chain and main-chain atoms are presented in Fig. 9. Taking into consideration all possible errors, it is obvious that the overall temperature factor does not depend on the temperature. This result indicates a strong increase in lattice disorder with shock freezing, since $\langle x^2\rangle_d$ must decrease as the temperature

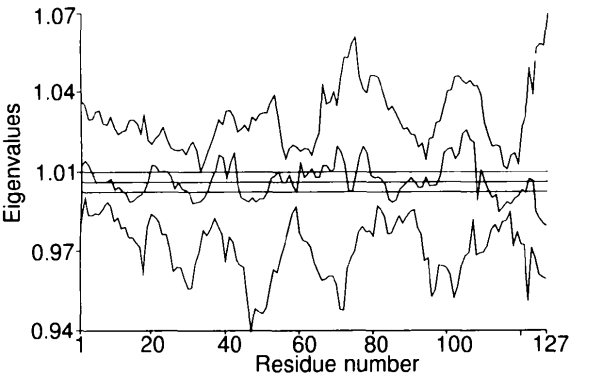

Fig. 8. Three eigenvalues of the strain tensor, plotted as a function of residue number, when a comparison of low- and high-temperature structure of lysozyme was performed. Straight lines show standard deviation from 1, assuming that small median eigenvalues are as a result of coordinate errors.

decreases. The temperature factor plotted against residue number (Fig. 10) is nearly independent of the temperature with a correlation factor near 0.9 for different data sets. The temperature-factor dependence for side-chain atoms also follows roughly the main-chain temperature factor with a correlation of 0.5–0.55 for LT and 0.4 for HT structures. These similarities strongly support the assumption that

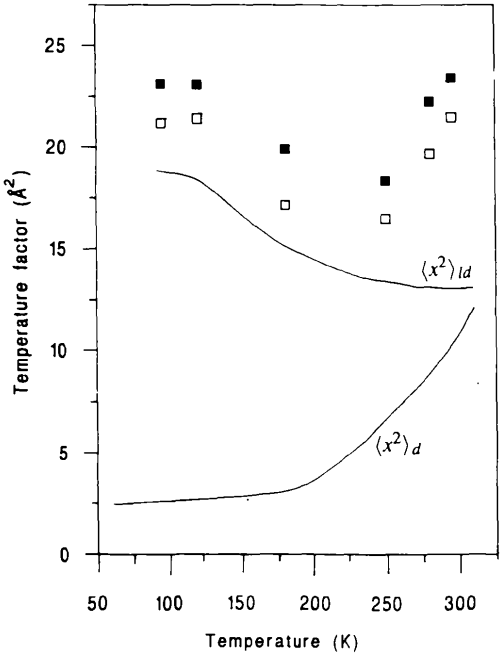

Fig. 9. The overall *B*-factor values for side-chain atoms, ■, and for main-chain atoms, □, as a function of the temperature. Two solid lines depict temperature dependences of $\langle x^2\rangle_{ld}$ and $\langle x^2\rangle_d$.

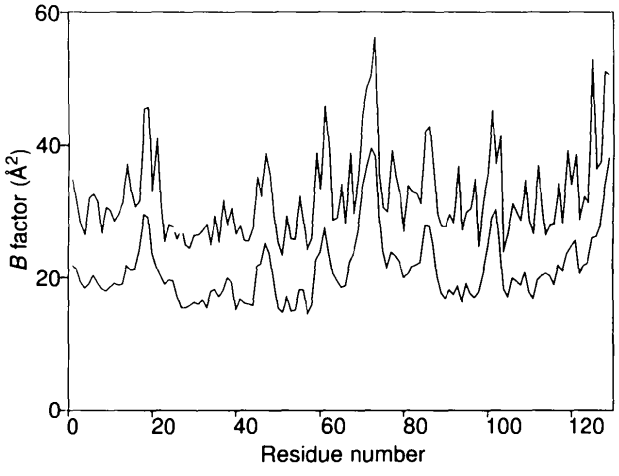

Fig. 10. Average *B* factor for main-chain atoms (lower curve) as a function of residue number for lysozyme at 95 K; upper curve, average *B* factor for side-chain atoms, shifted up for clarity by 10 Å².

$\langle x^2\rangle_{ld}$ varies only slightly along the polypeptide chain. We failed to find any correlation of temperature factor with accessible surface area (correlation less than 0.15) or with the distance of the center of residue from the center of protein, so the contribution of libration disorder is not significant. The overall behavior of temperature factor is correlated with the secondary-structure elements residues located in turns or at termini possess larger temperature factors. Many of these residues show increased temperature factors as the temperature decreased, for example, out of 32 residues which display increased temperature factors greater than 3 Å² on going from 280 to 95 K, only five are in secondary structure elements.

The overall temperature factor in HT is 21.7 Å², which corresponds to $\langle x^2\rangle = 0.28$ Å². It is possible to estimate the contribution of static lattice disorder to this value, if the data on lysozyme overall dynamics obtained by Rayleigh scattering of Mossbauer radiation (Kurinov, Krupianskii, Suzdalev & Goldanskii, 1987) are used. The method of Rayleigh scattering of Mossbauer radiation provides information only on $\langle x^2\rangle_d$ values of internal motions with correlation times less than 10^{-7} and it is free from any contribution from lattice disorder. It was shown that the hydration of lysozyme leads to the release of conformational mobility with $\langle x^2\rangle_d \simeq 0.10$ Å² in addition to usual solid-state oscillation with 0.04 Å². These values do not depend on the hydration degree in the range 0.35–0.7 g H_2O per g protein. Assuming that the dynamical mobility of protein in hydrated powder is close to that in the crystal state, it is possible to conclude that the overall contribution of lattice disorder at HT constitutes one half of the total $\langle x^2\rangle$, and has much higher value in LT, where $\langle x^2\rangle_d$ is near 0.03 Å².

In this study of temperature dependence of isotropic temperature factor it is impossible to obtain detailed information on protein dynamics because the method of shock freezing had led to increased lattice disorder. However the lattice disorder in these lysozyme crystals already accounts for approximately half of the thermal disorder at room temperature so that even under normal conditions such analysis is less than rigorous.

III. *Water structure and dynamics*

We now consider the structural and dynamical properties of crystalline water. During the refinement process only water molecules with temperature factors less than 50 Å² were considered, and they were placed to fit the highest electron-density peaks in difference maps only if they were near protein atoms. The occupancy factors for all water molecules were set to 1 and were not varied. At the end of

refinement some of waters had higher temperature factors (see Table 2) and had moved farther from protein. As the temperature decreased, a few more water molecules became visible in the refined structure (see Table 2). The ordered water molecules consitute only about 1/4 of all crystalline water [assuming the lysozyme crystal as a 33.5% protein solution (Steinrauf, 1959)]. Much of the solvent remains disordered, even at very low temperature, and has an amorphous structure that cannot be modeled by an atomic model. The overall temperature factor for water molecules with individual temperature factors less than 50 Å^2, is nearly independent of the temperature and lies in the range 31 ($\pm$2) Å^2. This again indicates the significant structural disorder of water at low temperatures. Nevertheless, some water molecules possess relatively low temperature factors near 10 Å^2.

During the molecular-dynamics calculations used in the structural refinement some water molecules had moved far from the protein and exchanged positions with symmetry-related waters. All water molecules (including symmetry-related ones) were considered in further analysis. Table 6 presents the number of waters and corresponding average temperature factors as a function of distance from the protein surface. The temperature factor increases as the distance of water molecules from the protein increases, and the majority of ordered waters are in the 4 Å shell. But that water amount is still insufficient to fully cover the protein surface, [even taking into account intermolecular protein contacts and assuming a 20 Å^2 covered surface from one hydrogen water molecule (Rupley *et al.*, 1983)]. An unusual effect is seen with the 280 K structure. The number of ordered waters in the nearest shell is smaller in this structure than in either the 295 or the 250 K structure. Those waters which ordered have comparable thermal factors to the higher and lower temperature structures.

The localization of water molecules around O and N atoms (as possible acceptors and donors of hydrogen bonds) in main chain and side chains at about 3.5 Å from the protein surface was analyzed. The results show the considerable and stable ordering of water near particular protein groups. The presence of stable water molecules near the same group in at least four different temperature structures was chosen as a definition of stable hydration. It was found that 40 carboxyl O atoms and 23 amide N atoms are constantly hydrated and also 59 O atoms and 32 N atoms of the main chain are hydrated at three different temperatures. The correlation of the hydration of main-chain atoms with secondary structure is not very pronounced: there are some waters near α-helices and β-sheets with only one exception of α-helical residues 24–35, which are buried inside

Table 6. *Number of water molecules in shells at different distances from protein surface and overall B factor* (Å) *for water in each shell*

	Distance from protein		
	Up to 3.0 Å	3.0–4.0 Å	4.0–6.0 Å
295 K	59	23	10
B factor	36.2	42.9	44.3
280 K	28	22	12
B factor	33.5	41.1	41.2
250 K	64	22	11
B factor	30.6	36.9	48.2
180 K	74	42	13
B factor	29.4	34.6	36.7
120 K	71	42	20
B factor	32.1	37.7	38.8
95 K	76	39	15
B factor	30.7	34.4	38.7

other secondary elements. The number of hydrated main-chain O atoms is only 74% more than the number of hydrated main-chain N atoms despite the two lone-pair electrons of O atoms. Nearly the same water ordering persists for side chains. Due to the higher temperature factors of terminal O and N atoms of side chains, the bound water in these regions also possesses higher temperature factors and, therefore, was not always obvious in the electron-density map. Of the 37 O and 22 N atoms that are hydrated at three different temperatures 23 and 15, respectively, are hydrated at four temperatures. The charged residues (Glu, Lys, Asp and Arg) have the highest hydration of up to three water molecules per residue. For side chains the number of ordered moelcules near O and N atoms slightly increased as the temperature decreased, probably due to the immobilization of the longer groups. However, main-chain hydration remains nearly temperature independent.

Table 7 gives the average hydrogen-bonding distances for all hydrating water molecules to O and N atoms for high- and low-temperature structures, taking into consideration only water molecules at 3.5 or 3.2 Å from protein atoms. Possible hydrogen bonds to N atoms are slightly longer by 0.1 Å and show more pronounced temperature dependence, compared to —C=O—O_{water} bonds. The interactions of main-chain atoms with water are stronger and more stable than for side-chain atoms, as reflected in the corresponding distances. The results in Table 7 are in good agreement with an analogous survey by Teeter (1991) and with similar data on other types of lysozyme (Blake *et al.*, 1983).

Table 8 gives the number of water molecules, which have 0, 1, 2, 3, 4 or more neighboring atoms in the shell of radius 3.5 Å. The relative distribution is nearly independent of the temperature and demonstrates the disordered nature of nearly 1/4 of total located water molecules, which possess only one or even no nearest neighbors. These relatively equal

Table 7. *Hydrogen-bonding distances with water molecules using a cutoff factor of* 3.5 Å *and, in parentheses, the same values with a cutoff of* 3.2 Å

Temperature range	Main chain N···O*W* (Å)	Main chain CO···O*W* (Å)	Side chain N···O*W* (Å)	Side chain O···O*W* (Å)	O*W*···O*W* (Å)
High temperature	3.15	2.96	3.12	3.02	3.04
	(2.94)	(2.86)	(2.96)	(2.85)	(2.91)
Low temperature	3.09	2.95	3.07	3.02	2.94
	(2.95)	(2.83)	(2.91)	(2.89)	(2.85)

Table 8. *Number of water molecules around protein, having* 0, 1, 2, 3, 4 *or more neighboring atoms at a distance of less than* 3.5 Å

	Number of neighboring atoms						
Temperature (K)	0	1	2	3	4	>5	Average
95	7	18	30	34	13	6	2.65
120	4	25	27	23	13	12	2.57
180	6	18	28	26	12	14	2.67
280	3	9	11	10	–	6	2.38
250	0	8	22	28	12	13	2.76
295	6	13	19	12	12	11	2.51

numbers of water neighbors at high and low temperatures are a good illustration of the transition from dynamical to statical disorder of the water pool. The average number of neighbors around each water molecule near the protein surface was estimated to be nearly the same at all temperatures. For the waters with four and more neighbors, the 'clusters' of neighboring atoms are very stable and are located practically at the same position near charged side chains and are present in all of our structures. An attempt to find a stable pure water 'cluster' was unsuccessful: only random water formations with four waters inside a 4.5 Å sphere were found.

Concluding remarks

The influence of temperature on the structural and dynamical properties of lysozyme crystals in the range 95–295 K has been analyzed. Lowering temperature leads to a 7.4% decrease of unit-cell volume, which is non-linear with a discontinuity in the range 200–240 K. The protein volume decreases about 2.5%, based on the radius-of-gyration calculations, and is accompanied by an increase of short-range interatomic distances. It was determined that protein thermal contraction is anisotropic and is determined by local atomic packing and by relative motions of secondary-structure elements. The overall result of unit-cell shrinkage is a translation and a rotation of the protein as a whole, associated with some surface-water rearrangements and local conformational changes of protein side-chains involved in intermolecular contacts. However, the overall structure of lysozyme at low temperature remains nearly the same as at higher temperature; only relatively small pivoting of secondary-structure elements occurs. Many local differences were found in the regions outside the secondary-structure elements. A hinge-bending motion of the two lysozyme domains was seen: at low temperature the two domains are drawn together.

The method of shock freezing leads to a considerable increase of lattice disorder as measured by temperature factors. This complicated the dynamical analysis of internal motion. Dynamical disorders of protein groups and water molecules at high temperatures are transformed into static disorder at low temperatures, as indicated by the temperature independence of the overall temperature factors. Consideration of Mössbauer data on hydrated lysozyme allowed an estimate of lattice disorder at room temperature of one half of the overall temperature factor and a much higher value at low temperatures. A short analysis of structure and dynamics of well ordered water was undertaken. A temperature decrease leads to a small increase in the number of hydrating water molecules which can be fitted with an atomic model. These water molecules constitute only 1/4 of all possible waters, even at low temperature, and are insufficient to cover the whole protein surface. The hydration of main-chain O atoms and N atoms was found to be nearly temperature independent and stable. The average distances between water O atoms and possible donor and acceptor atoms were determined. Water molecules near the protein surface have about 2.6 nearest neighbors. No stable ordered water formations were found in solvent region.

In subsequent low-temperature X-ray crystallography of protein structure and dynamics, greatest attention must be paid to selection of the best experimental methodology of sample preparations. First of all, a considerable decrease of lattice disorder is very valuable, since a distribution of alternative conformations of protein groups might be analyzed and much more ordered water molecules can be extracted from less noisy electron-density maps. Moreover, it is worthwhile to carefully examine the 180–240 K region, to have the opportunity of direct observation of structural–dynamical relationships connected with melting of hydration water and the appearance of intramolecular conformational mobility in the protein.

The authors are grateful to Jill Verfaillie and Jin Wu for technical assistance.

References

ANDREWS, L. C. & HARRISON, R. W. (1991). *Proteins Struct. Funct. Genet.* **10**, 162–170.

ARTYMIUK, P. J., BLAKE, C. C. F., GRACE, D. E. P., OATLEY, S. J., PHILLIPS, D. C. & STENBERG, M. J. E. (1979). *Nature (London)*, **280**, 563–568.

BERNSTEIN, F. C., KOETZLE, T. F., WILLIAMS, G. J. B., MEYER, E. F. JR, BRICE, M. D., RODGERS, J. R., KENNARD, O., SHIMANOUCHI, T. & TASUMI, M. (1977). *J. Mol. Biol.* **112**, 535–542.

BLAKE, C. C. F., KOENIG, D. F., MAIR, G. A., NORTH, A. C. T., PHILLIPS, D. C. & SARMA, V. R. (1965). *Nature (London)*, **206**, 757–761.

BLAKE, C. C. F., PULFORD, W. C. A. & ARTYMIUK, P. J. (1983). *J. Mol. Biol.* **167**, 696–723.

BRÜNGER, A. T. (1992*a*). *X-PLOR* Version 3.0 *Manual.* Yale Univ., New Haven, Connecticut, USA.

BRÜNGER, A. T. (1992*b*). *Nature (London)*, **355**, 472–474.

BRÜNGER, A. T., KRUKOVSKII, A. & ERICKSON, J. W. (1990). *Acta Cryst.* A**46**, 585–593.

BULL, H. B. & BREESE, K. (1973). *Biopolymers*, **12**, 2351–2358.

CLARAGE, J. B., CLARAGE, M. S., PHILLIPS, W. C., SWEET, R. M. & CASPAR, D. L. D. (1992). *Protein Struct. Funct. Genet.* **12**, 145–157.

DEWAN, J. C. & TILTON, R. F. (1987). *J. Appl. Cryst.* **20**, 130–132.

DOSTER, W., CUSACK, S. & PETRY, W. (1989). *Nature (London)*, **337**, 754–756.

FRAUENFELDER, H., HARTMANN, H., KARPLUS, M., KUNTZ, I. D. JR, KURIYAN, J., PARAK, F., PETSKO, G. A., RINGE, D., TILTON, R. F. JR, CONNOLLY, M. L. & MAX, N. (1987). *Biochemistry*, **26**, 254–261.

FRAUENFELDER, H., PARAK, F. & YOUNG, R. (1988). *Annu. Rev. Biophys. Biophys. Chem.* **17**, 451–459.

HARTMANN, H., PARAK, F., STEIGEMANN, W., PETSKO, G. A., RINGE, D. & FRAUENFELDER, H. (1982). *Proc. Natl Acad. Sci. USA*, **79**, 4967–4971.

HOPE, H. (1988). *Acta Cryst.* B**44**, 22–26.

HOPE, H. (1990). *Annu. Rev. Biophys. Biophys. Chem.* **19**, 107–126.

JANIN, J. & WODAK, S. J., (1983). *Prog. Biophys. Mol. Biol.* **42**, 21–78.

JONES, T. A. (1985). *Methods Enzymol.* **115**, 157–171.

KRUPYANSKII, YU, F., GOLDANSKII, V. I., KURINOV, I. V. & SUZDALEV, I. P. (1990). *Stud. Biophys.* **136**, 133–148.

KUNDROT, C. E. & RICHARDS, F. M. (1987). *J. Mol. Biol.* **193**, 157–170.

KURINOV, I. V., KRUPIANSKII, YU, F., SUZDALEV, I. P. & GOLDANSKII, V. I. (1987). *Hyperfine Interactions*, **33**, 223–232.

KURIYAN, J., KARPLUS, M. & PETSKO, G. A. (1987). *Proteins Struct. Funct. Genet.* **2**, 1–12.

KURIYAN, J., PETSKO, G. A., LEVY, R. M. & KARPLUS, M. (1986). *J. Mol. Biol.* **190**, 227–254.

KURIYAN, J. & WEIS, W. I. (1991). *Proc. Natl Acad. Sci. USA*, **88**, 2773–2777.

LUZZATI, V. (1952). *Acta Cryst.* **5**, 802–810.

MCKENZIE, H. A. & WHITE, F. H. (1991). *Adv. Protein Chem.* **41**, 174–315.

PETSKO, G. A. (1975). *J. Mol. Biol.* **96**, 381–392.

PETSKO, G. A. & RINGE, D. (1984). *Annu. Rev. Biophys. Bioeng.* **13**, 331–371.

RUPLEY, J. A. & CARERI, G. (1991). *Adv. Protein Chem.* **41**, 37–172.

RUPLEY, J. A., GRATTON, E. & CARERI, G. (1983). *Trends Biochem. Sci.* **8**, 18–22.

STEINRAUF, L. K. (1959). *Acta Cryst.* **12**, 77–79.

TEETER, M. M. (1991). *Annu. Rev. Biophys. Chem.* **20**, 577–600.

TILTON, R. F. JR, DEWAN, J. C. & PETSKO, G. A. (1992). *Biochemistry*, **31**, 2469–2481.

YOUNG, A. C. M., DEWAN, J. C., THOMSON, A. W. & NAVE, C. (1990). *J. Appl. Cryst.* **23**, 215–218.